

Energy-energy correlations on tracks: factorization and resummation

Max Jaarsma,^{a,b} Yibei Li,^{c,*} Ian Moutl,^d Wouter Waalewijn^{a,b} and Hua Xing Zhu^e

^a*Nikhef, Theory Group,
Science Park 105, 1098 XG, Amsterdam, The Netherlands*

^b*Institute for Theoretical Physics Amsterdam and Delta Institute for Theoretical Physics, University of
Amsterdam, Science Park 904, 1098 XH Amsterdam, The Netherlands*

^c*Zhejiang Institute of Modern Physics, School of Physics, Zhejiang University,
Hangzhou, 310027, China*

^d*Department of Physics, Yale University,
New Haven, CT 06511, USA*

^e*School of Physics, Peking University,
Beijing 100871, China*

*E-mail: m.jaarsma@uva.nl, aisijimoren@zju.edu.cn, ian.moutl@yale.edu,
w.j.waalewijn@uva.nl, zhuhx@pku.edu.cn*

To do experimentally clean measurements, one of the proposed strategies is to use track-based observables, which means working exclusively with final-state charged hadrons (tracks). The field-theoretic framework introduced to calculate track-based observables is the so-called track function formalism. Although the case of most experimental interest is track, this framework, based on the factorization and universality of collinear divergences, can be applied to measurements on any subset of final-state hadrons with a set of particular quantum numbers. While the track function formalism has existed for eleven years, it is just in the past few years that we have extended it beyond leading order, making it practical in higher-order calculations comparable to experimental data. We illustrate its power by probing into the kinematic singularities of energy correlators on tracks: we calculate the projected two- to six-point energy correlators on tracks in the collinear limit at next-to-leading logarithmic (NLL) accuracy; we give the factorization theorem for the track energy-energy correlation (EEC) observable in the back-to-back limit, and compute the track EEC at next-to-leading logarithm (NLL). This leads to the first full prediction of the track EEC in perturbation theory, making the track correlator a prime candidate for precision QCD studies.

*Loops and Legs in Quantum Field Theory (LL2024)
14-19, April, 2024
Wittenberg, Germany*

*Speaker

1. Introduction

In the past few years, there has been growing interest in applying energy correlators to probe into both perturbative and nonperturbative QCD in vacuum and medium. The significance of the comparison between theory and experimental data relies on the precision that the calculations and measurements of interesting signals achieve. In perturbation theory, for the phase space where collinear and/or soft radiation dominate, it is crucial to do resummation to high accuracy for the logarithmically enhanced contributions. From the perspective of collider experiments, due to the exceptional efficiency and precision of trackers, track-based observables that are reconstructed from the kinematics of final-state charged particles (tracks) can be measured with superior resolution and reduce the effect of pileup, which helps in the measurements strongly relying on angular resolution, like jet substructure.

Our work is a combination of modern techniques for fixed-order calculations and resummation, and a field-theoretic scheme for calculations exclusively on a subset of final-state hadrons.

2. Energy correlators

The k -point energy correlator is defined as a correlation function of k energy flow operators,

$$\langle \mathcal{E}(\vec{n}_1) \cdots \mathcal{E}(\vec{n}_k) \rangle \equiv \frac{\langle 0 | \mathcal{O}^\dagger \mathcal{E}(\vec{n}_1) \cdots \mathcal{E}(\vec{n}_k) \mathcal{O} | 0 \rangle}{\langle 0 | \mathcal{O}^\dagger \mathcal{O} | 0 \rangle} \quad (1)$$

where the energy flow operator $\mathcal{E}(\vec{n})$,

$$\begin{aligned} \mathcal{E}(\vec{n}) &= \lim_{r \rightarrow \infty} r^2 \int_0^\infty dt \vec{n}^i T_{0i}(t, r\vec{n}), \\ \mathcal{E}(\vec{n}) | X \rangle &= \sum_a p_a^0 \delta^{(2)}(\Omega_{\vec{p}_a} - \Omega_{\vec{n}}) | X \rangle, \end{aligned} \quad (2)$$

measures the total, asymptotic energy per unit solid angle at the direction \vec{n} [1–5]. In this way, the k -point energy correlator evaluates the energy fluxes measured by k detectors placed distant from the collision. It depends on $\binom{k}{2} = k(k-1)/2$ independent angular variables. For the sake of experimental convenience, the projected k -point energy correlators have been introduced, and here we focus on the longest side definition [5], which means integrating energy correlators over all variables about shape except the longest side (i.e., the largest angular size, x_L),

$$\frac{d\sigma^{[k]}}{dx_L} = \int d\vec{\Omega} \delta\left(x_L - \frac{1 - \vec{n}_1 \cdot \vec{n}_2}{2}\right) \prod_{\substack{1 \leq i < j \leq k \\ i+j > 3}} \Theta(|\vec{n}_1 - \vec{n}_2| - |\vec{n}_i - \vec{n}_j|) \langle \mathcal{E}(\vec{n}_1) \cdots \mathcal{E}(\vec{n}_k) \rangle. \quad (3)$$

The energy correlators have a number of interesting features. First, the soft contributions are suppressed due to the energy weighting. This soft insensitivity renders the energy correlators single-logarithmic (soft insensitive) in the collinear limit. Second, the energy correlators are arguably the simplest class of energy flow observables. They're the only event shapes that have been fully calculated analytically beyond $\mathcal{O}(\alpha_s)$ [6–10]. Although energy correlators have perturbative simplicity, their interesting kinematic singularities are not obscured. One usually uses the factorization theorems and renormalization group (RG) techniques to resum the large logarithms in the

singular regions (the collinear limit and the back-to-back limit). For example, in the two-point case, also called energy-energy correlation (EEC) with the definition that phenomenologists usually use reading [6]

$$\frac{d\sigma}{dx_L} \equiv \sum_m \sum_{1 \leq i, j \leq m} \int d\Phi_m |\mathcal{M}_m|^2 \frac{E_i E_j}{Q^2} \delta \left(x_L - \frac{1 - \cos \chi_{ij}}{2} \right), \quad (4)$$

the angular distance $x_L \rightarrow 0$ corresponds to the angle of the two observed particles $\chi_{ij} \rightarrow 0$, which means the two energy flow operators are evaluated at very similar directions. This is the collinear limit. And $x_L \rightarrow 1$ corresponds to the two particles being back-to-back, which is the Sudakov region [11, 12].

In the collinear limit, the energy correlators have further features. In the following we focus on the projected N -point energy correlators ($N \in \mathbb{N}_+$) in the $x_L \rightarrow 0$ limit which refers to that all the energy flow operators, or say detectors, are set at closely matching angles. This allows us to probe into the energy correlators within a jet. In the perturbative region, the projected N -point correlator exhibits a universal scaling behaviour controlled by the twist-two spin- $N + 1$ anomalous dimensions, that is, $x_L^{\gamma(N+1, \alpha_s)}/x_L$ [5, 13, 14]. While this formula holds strictly in $\mathcal{N} = 4$ super Yang-Mills theory (SYM), it's an approximate relation in real-world QCD. For example, for the EEC in QCD, its dependence on the angular distance x_L is all encoded in the classical scaling $1/x_L$ and the OPE coefficients (see Eq. (3.16) in Ref. [15]¹). Besides the scaling for the perturbative region, the projected energy correlators exhibit the ability to conveniently visualize hadronization process inside jets [16–21]. By the change in scaling behaviour, one can clearly see the transition from perturbatively interacting quarks and gluons to free hadrons.

The back-to-back energy-energy correlation on all particles has been studied in Refs. [11, 12], where the factorization formulas and the resummation to N3LL' have been achieved. Experimental measurements probing into this region have started.

3. Incorporating track functions

3.1 Definition of track functions

The aforementioned energy flow observables act on all final-state particles. On the other hand, one can select what group of particles to observe by their charge, strangeness, or any other pieces of information of quantum numbers, which means observing a subset of final state particles. This makes the correlations of energy flows be a more exclusive observable with extra quantum number information. The example of most experimental interest is track-based observable reconstructed from charged particles. High energy jets in hadron colliders require small-angle measurements and thus surely benefit from the exceptional angular resolution of tracking system.

To make theoretical predictions on a subset R of final-state particles, the track function was introduced [22, 23]. Based on the collinear factorization theorem [24], the track function is a universal nonperturbative function, and can absorb partonic-level collinear divergences, behaving in the way similar to fragmentation functions. It is a probability distribution function, usually denoted by T . $T_i(x)$ describes the probability density of finding in a jet initiated by an energetic

¹Note that in Ref. [15], x_L is denoted by z .

parton i the particles in the subset R (having a set of particular quantum numbers) with the total momentum fraction x . Because the subset of most experimental interest is that of charged particles, the track function is named after track. So in this paper, all the plots are made for the charged particle case, while our framework applies to broader situations other than observables on tracks. In the following, we use the subset R and track interchangeably.

The operator definition of the quark track function in light-cone gauge reads [22, 23, 25–28]

$$T_q(x) = \int dy^+ d^2 y_\perp e^{ik^- y^+ / 2} \frac{1}{2N_c} \sum_{R, \bar{R}} \delta\left(x - \frac{P_R^-}{k^-}\right) \text{tr} \left[\frac{\gamma^-}{2} \langle 0 | \psi(y^+, 0, y_\perp) | R \bar{R} \rangle \langle R \bar{R} | \bar{\psi}(0) | 0 \rangle \right], \quad (5)$$

with the gluon track function defined in a similar way. To get a gauge-invariant definition in general covariant gauges, Wilson line is required. As one may see from the definition, the track function describes the total kinematics of a set of particles with no limit on the number, and thus the evolution equation of track functions tracks all the momentum fractions of a collinear splitting at a time, while the DGLAP equation of single-hadron fragmentation functions tracks one of the partonic branchings at a time. This leads to the nonlinearity of the track function renormalization group evolution (RGE).

3.2 Energy correlators on tracks

To convert an energy correlator on all final-state particles to that on tracks is to convert the energy flow operators measuring energy flows on all final states to that only on tracks, here denoted by \mathcal{E}_R . The correlator on tracks and the partonic level one are connected by moments of track functions through a factorization formula [26],

$$\langle \mathcal{E}_R(\vec{n}_1) \mathcal{E}_R(\vec{n}_2) \cdots \mathcal{E}_R(\vec{n}_k) \rangle = \sum_{a_1, a_2, \dots, a_k} T_{a_1}(1) T_{a_2}(1) \cdots T_{a_k}(1) \langle \mathcal{E}_{a_1}(\vec{n}_1) \mathcal{E}_{a_2}(\vec{n}_2) \cdots \mathcal{E}_{a_k}(\vec{n}_k) \rangle + [\text{contact terms}], \quad (6)$$

and the moments, as nonperturbative numbers, do not take part in the phase space integration, which allows us, at any loop order, to directly apply perturbative calculation techniques to calculations on tracks.

4. Collinear limit

In the collinear limit, the projected N -point energy correlator on tracks factorizes into a hard function and a jet function describing angular measurements with the dependence on track function moments [18],

$$\left(\frac{d\Sigma^{[N]}}{dx_L} \right)_{\text{tr}} = \vec{H} \otimes \vec{J}_{\text{tr}}^{[N]}, \quad (7)$$

where the hard function \vec{H} and the jet function $\vec{J}_{\text{tr}}^{[N]}$ are in flavour space. Due to the difference between the hard scale $\sim Q$ and the jet scale $\sim \sqrt{x_L} Q$, the collinear correlator has large logarithms which can be resummed by RG evolution:

$$\text{LL: } \alpha_s^l \left[\frac{\ln^{l-1} x_L}{x_L} \right]_+, \quad \text{NLL: } \alpha_s^l \left[\frac{\ln^{l-2} x_L}{x_L} \right]_+, \quad \text{NNLL: } \alpha_s^l \left[\frac{\ln^{l-3} x_L}{x_L} \right]_+. \quad (8)$$

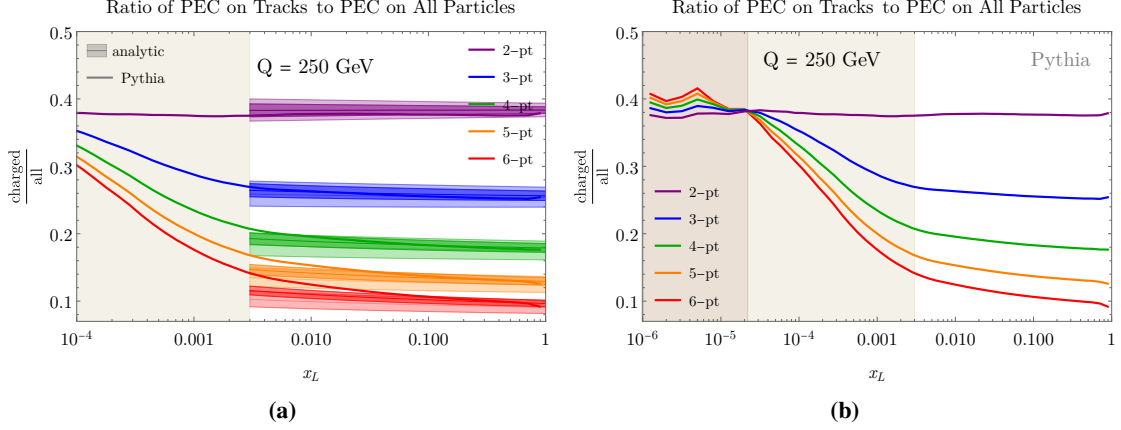


Figure 1: The ratio of the projected energy correlators (PEC) computed on charged hadrons vs. all hadrons. (a) Results from PYTHIA, and analytic predictions at LL and NLL. (b) Results from PYTHIA.

We achieve the NLL resummation for the projected up to six-point energy correlators on tracks, and find that in the perturbative region, the scaling behaviour is modified by the logarithmic running of the track function moments [18]. In Fig. 1, we take the ratio of the projected energy correlator on tracks to that on all particles, for the two- to six-point cases in e^+e^- , as a comparison between the all and charged particle cases. The darker bands correspond to the NLL resummed predictions, and the lighter bands correspond to the LL resummation, while the solid lines are the Pythia data. Due to the convention we choose to scale energy weights (E/Q with the particle energy E and the c.o.m energy Q in e^+e^-), the N -point result ($N = 2, 3, 4, 5, 6$) in the plot has an overall factor $\sim T(k)T(N-k)$.

As shown in Fig. 1a, in the perturbative region (right, with the background color being white), the anomalous dimensions of track functions impose a perturbatively predictable modification on the scaling behaviour: with the track information introduced, the scaling law, $\sim x_L^{\gamma(N+1, \alpha_s)}/x_L$ for the all-particle case, is changed to $\sim x_L^{\gamma_{\text{tr}}(N+1, \alpha_s)}/x_L$ in the track case, where $\gamma_{\text{tr}}(N+1, \alpha_s) \approx \gamma(N+1, \alpha_s) - \delta(N+1, \alpha_s)$ with $\delta(N+1, \alpha_s)$ resulting from the effect of the N -th moments of track function anomalous dimensions, \widehat{R}_N . Although $\gamma_{\text{tr}}(N+1, \alpha_s)$ and \widehat{R}_N are usually not in the same space², naively and roughly we have $\delta(N+1, \alpha_s) \sim -\widehat{R}_N$. Then, $\delta(N+1, \alpha_s)$ is to a large extent controlled by the twist-2 spin- $N+1$ anomalous dimensions. Thus, $\gamma_{\text{tr}}(N+1, \alpha_s) \lesssim \gamma(N+1, \alpha_s)$, which leads to the decreasing behaviour as x_L gets larger. For the two- and three-point cases, the curves in the perturbative region are very flat, which means that including tracks barely changes the shapes. This results from the cancellations in nonperturbative track function moments and then in their evolution. For the higher point cases, the incorporation of track information has larger effects. The higher moments of track functions have faster evolution.

Fig. 1b shows the Pythia data covering the collinear limit from the perturbative region to the free hadron region (left, dark shaded). The value of the ratio in the free hadron region is the probability of finding two of the particles charged, which is approximately $(2/3)^2 \approx T(1)^2$. The

² \widehat{R}_N is in the track function moment space. See Refs. [18, 26].

curves in the transition region (middle, shaded) connect the curves in the perturbative region to those in the free hadron region. This explains the flat behaviour of the two-point case for the whole range.

5. Back-to-back limit

In the back-to-back limit, we focus on the $E^{m_1}E^{m_2}C$ on R (e.g., tracks, and all particles) in e^+e^- , which is defined as two back-to-back particles with the energy weighting E^{m_1} and E^{m_2} respectively. Following the factorization theorem in di-hadron production in Ref. [29], We find that the back-to-back $E^{m_1}E^{m_2}C$ factorizes into the hard function H , the back-to-back jets J 's, and the soft function S ³:

$$\begin{aligned} \frac{d\sigma}{dz}^{[m_1, m_2]} &= \frac{\hat{\sigma}_0}{2} \int d^2\vec{q}_T \delta\left(1 - z - \frac{q_T^2}{Q^2}\right) \int \frac{d^2\vec{b}_T}{(2\pi)^2} e^{-i\vec{q}_T \cdot \vec{b}_T} H_{q\bar{q}}(Q, \mu) \tilde{S}_q(b_T, \mu, \nu) \\ &\quad \times J_R^{[m_1], q}\left(b_T, \mu, \frac{\nu}{Q}\right) J_R^{[m_2], q}\left(b_T, \mu, \frac{\nu}{Q}\right), \end{aligned} \quad (9)$$

where the quark jet function on R reads

$$J_R^{[m], q}\left(b_T, \mu, \frac{\nu}{Q}\right) = \sum_i \int_0^1 dx x^m \mathcal{I}_{qi}\left(\frac{b_T}{x}, x, \mu, \nu\right) \mathcal{F}_i(m, \mu), \quad (10)$$

where the m -th moment of fragmentation functions on R is defined as

$$\mathcal{F}_i(m, \mu) \equiv \sum_{I \in R} \int dz z^m f_{i \rightarrow I}(z, \mu) \quad (11)$$

with if $m = 1$

$$\mathcal{F}_i(1, \mu) = T_i(1, \mu). \quad (12)$$

$\mathcal{I}_{qi}\left(\vec{b}_\perp/x, x, \mu, \nu\right)$ is the matching coefficient of transverse-momentum-dependent fragmentation functions (TMD FFs)[30], and $f_{i \rightarrow I}(z, \mu)$ is the collinear fragmentation function. Note that for the all-hadron case, Eq. (12) equals one due to the momentum conservation, so the collinear fragmentation functions do not enter in Eq. (9) with $m_1 = m_2 = 1$, which indicates that EEC is infrared safe.

The renormalization group equations for the different pieces in the factorization formula Eq. (9) remain the same as the all-particle EEC case. We evolve the hard, jet and soft functions via their RGEs from their natural scales to a common scale μ ,

$$\begin{aligned} \frac{d\sigma}{dz}^{[m_1, m_2]} &= \frac{\hat{\sigma}_0}{8} \int_0^\infty d(b_T Q)^2 J_0(b_T Q \sqrt{1-z}) H_{q\bar{q}}(Q, \mu_H) \\ &\quad \times J_R^{[m_1], q}\left(b_T, \mu_J, \frac{\nu_J}{Q}\right) J_R^{[m_2], q}\left(b_T, \mu_J, \frac{\nu_J}{Q}\right) \tilde{S}_q(b_T, \mu_S, \nu_S) \left(\frac{\nu_J}{\nu_S}\right)^{\tilde{\gamma}_q^q(b_T, \mu)} \\ &\quad \times \exp\left[\int_{\mu_H}^\mu \frac{d\mu'}{\mu'} \gamma_H^q(Q, \mu') + 2 \int_{\mu_J}^\mu \frac{d\mu'}{\mu'} \tilde{\gamma}_J^q(\mu', \frac{\nu_J}{Q}) + \int_{\mu_S}^\mu \frac{d\mu'}{\mu'} \tilde{\gamma}_S^q(\mu', \nu_S)\right], \end{aligned} \quad (13)$$

³Note that for cases where $J_R^{[m], q} \neq J_R^{[m], \bar{q}}$, the exchange of m_1 and m_2 ($m_1 \neq m_2$) should be considered. But this extension is straightforward. Here for notational simplicity, we assume $J_R^{[m], q} = J_R^{[m], \bar{q}}$. x_L is denoted by z here.

where we follow the notation in Ref. [12] and the canonical resummation scales read

$$\mu_H \sim Q, \mu_J \sim \frac{b_0}{b_T^*(b_T)}, \mu_S \sim \frac{b_0}{b_T^*(b_T)}, \mu_0 \sim \frac{b_0}{b_T^*(b_T)}, \nu_J \sim Q, \nu_S \sim \frac{b_0}{b_T} \quad (14)$$

with $b_{\max} = 1.5 \text{ GeV}^{-1}$. Finally we choose μ around the hard scale Q .

In Eq. (13), the jet functions contain $f_{i \rightarrow I}(m, \mu_J = b_0/b_T)$. In order to do the integration over b_T conveniently, we expand $\mathcal{F}_i(m, \mu_J = b_0/b_T)$ around the common scale μ : for NLL, $\vec{\mathcal{F}}(m, \mu_J) = \left[\frac{a_s(\mu_J)}{a_s(\mu)} \right]^{\gamma^{(0)}(m+1)/\beta_0} \vec{\mathcal{F}}(m, \mu)$ is introduced.

6. Full results of track EEC

Here we present the full distribution of track EEC, covering the aforementioned pieces of the different phase space regions. Fig. 2 shows the two-loop prediction (NLO), the NLO combined with the collinear NLL resummation, and the NLO combined with the back-to-back NLL' resummation, as well as the Pythia data. In both the collinear NLL and NLO results the uncertainty is evaluated by varying the common renormalization scale μ by a factor of 1/2 or 2, while for the back-to-back NLL', we evaluate its resummation scale following Ref. [12]. The straight-line behaviour in the extremely back-to-back region (right of the plot) tells us that the track EEC exhibits a similar scaling (free-hadron) characteristic to that in the deep nonperturbative region of the collinear limit (left of the plot). From Fig. 2a to Fig. 2c, as the c.o.m energy goes higher, the uncertainty bands become narrower, and the theoretical predictions become closer to the Pythia simulation. However, obviously the NNLL resummation is required to achieve a more precise prediction in the collinear limit.

We leave the results with higher accuracy and further detailed evaluation of uncertainties to a forthcoming paper, and the $E^{m_1}E^{m_2}C$ calculations to future work.

Acknowledgments

We thank Hao Chen for many useful discussions and collaboration on related topics. We thank Kyle Lee for helpful discussions. Y.L. and H.X.Z. are supported by the National Natural Science Foundation of China under contract No. 11975200. M.J. is supported by NWO projectruimte 680-91-122. I.M. is supported by start up funds from Yale University. W.W. is supported by the D-ITP consortium, a program of NWO that is funded by the Dutch Ministry of Education, Culture and Science (OCW).

References

- [1] C. L. Basham, L. S. Brown, S. D. Ellis, and S. T. Love, *Electron - Positron Annihilation Energy Pattern in Quantum Chromodynamics: Asymptotically Free Perturbation Theory*, *Phys. Rev. D* **17** (1978) 2298.
- [2] C. L. Basham, L. S. Brown, S. D. Ellis, and S. T. Love, *Energy Correlations in Perturbative Quantum Chromodynamics: A Conjecture for All Orders*, *Phys. Lett. B* **85** (1979) 297–299.

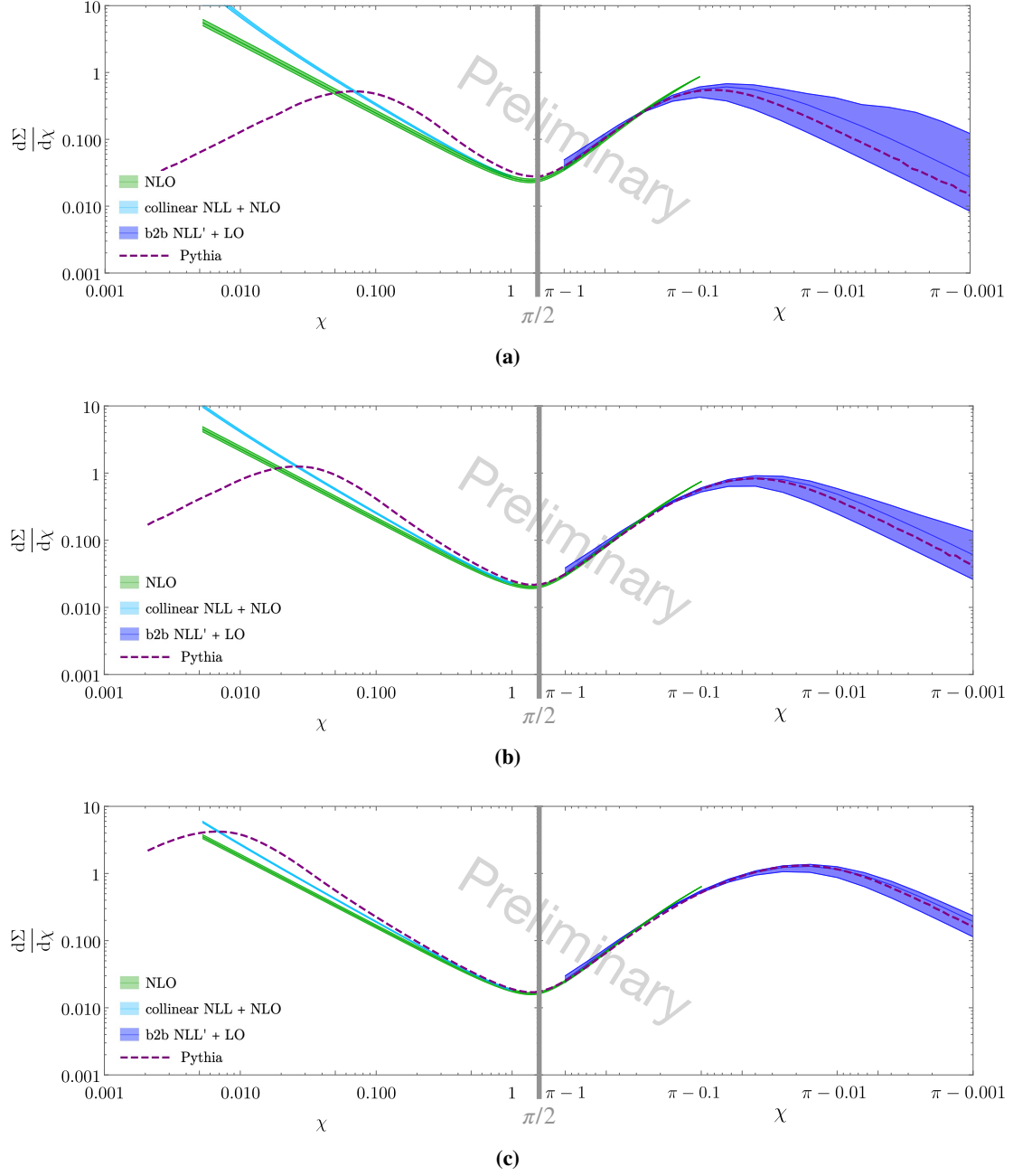


Figure 2: The full track EEC with the c.o.m energy $Q = 91.2$ GeV in (a), $Q = 250$ GeV in (b) and $Q = 1000$ GeV in (c).

- [3] N. Sveshnikov and F. Tkachov, *Jets and quantum field theory*, *Phys. Lett. B* **382** (1996) 403–408, [[hep-ph/9512370](#)].
- [4] A. V. Belitsky, G. P. Korchemsky, and G. F. Sterman, *Energy flow in QCD and event shape functions*, *Phys. Lett. B* **515** (2001) 297–307, [[hep-ph/0106308](#)].
- [5] H. Chen, I. Moulton, X. Zhang, and H. X. Zhu, *Rethinking jets with energy correlators: Tracks, resummation, and analytic continuation*, *Phys. Rev. D* **102** (2020), no. 5 054012, [[arXiv:2004.11381](#)].
- [6] L. J. Dixon, M.-X. Luo, V. Shtabovenko, T.-Z. Yang, and H. X. Zhu, *Analytical Computation of Energy-Energy Correlation at Next-to-Leading Order in QCD*, *Phys. Rev. Lett.* **120** (2018), no. 10 102001, [[arXiv:1801.03219](#)].
- [7] K. Yan and X. Zhang, *Three-Point Energy Correlator in $N=4$ Supersymmetric Yang-Mills Theory*, *Phys. Rev. Lett.* **129** (2022), no. 2 021602, [[arXiv:2203.04349](#)].
- [8] T.-Z. Yang and X. Zhang, *Analytic Computation of three-point energy correlator in QCD*, *JHEP* **09** (2022) 006, [[arXiv:2208.01051](#)].
- [9] A. Belitsky, S. Hohenegger, G. Korchemsky, E. Sokatchev, and A. Zhiboedov, *Energy-Energy Correlations in $N=4$ Supersymmetric Yang-Mills Theory*, *Phys. Rev. Lett.* **112** (2014), no. 7 071601, [[arXiv:1311.6800](#)].
- [10] J. Henn, E. Sokatchev, K. Yan, and A. Zhiboedov, *Energy-energy correlation in $N=4$ super Yang-Mills theory at next-to-next-to-leading order*, *Phys. Rev. D* **100** (2019), no. 3 036010, [[arXiv:1903.05314](#)].
- [11] I. Moulton and H. X. Zhu, *Simplicity from Recoil: The Three-Loop Soft Function and Factorization for the Energy-Energy Correlation*, *JHEP* **08** (2018) 160, [[arXiv:1801.02627](#)].
- [12] M. A. Ebert, B. Mistlberger, and G. Vita, *The Energy-Energy Correlation in the back-to-back limit at N^3LO and N^3LL'* , *JHEP* **08** (2021) 022, [[arXiv:2012.07859](#)].
- [13] L. J. Dixon, I. Moulton, and H. X. Zhu, *Collinear limit of the energy-energy correlator*, *Phys. Rev. D* **100** (2019), no. 1 014009, [[arXiv:1905.01310](#)].
- [14] K. Lee, B. Meçaj, and I. Moulton, *Conformal Colliders Meet the LHC*, [[arXiv:2205.03414](#)].
- [15] H. Chen, *QCD factorization from light-ray OPE*, *JHEP* **01** (2024) 035, [[arXiv:2311.00350](#)].
- [16] P. T. Komiske, I. Moulton, J. Thaler, and H. X. Zhu, *Analyzing N -Point Energy Correlators inside Jets with CMS Open Data*, *Phys. Rev. Lett.* **130** (2023), no. 5 051901, [[arXiv:2201.07800](#)].
- [17] **CMS Collaboration**, *Measurement of energy correlators inside jets and determination of the strong coupling constant*, .

- [18] M. Jaarsma, Y. Li, I. Moutl, W. J. Waalewijn, and H. X. Zhu, *Energy correlators on tracks: resummation and non-perturbative effects*, *JHEP* **12** (2023) 087, [[arXiv:2307.15739](#)].
- [19] **STAR** Collaboration, A. Tamis, *Measurement of Two-Point Energy Correlators Within Jets in $p p$ Collisions at $\sqrt{s} = 200$ GeV at STAR*, *PoS HardProbes2023* (2024) 175, [[arXiv:2309.05761](#)].
- [20] R. Cruz-Torres, *Measurement of the angle between jet axes and energy-energy correlators with ALICE*, *Hard Probes 2023*.
- [21] **CMS** Collaboration, A. Hayrapetyan et al., *Measurement of energy correlators inside jets and determination of the strong coupling $\alpha_S(m_Z)$* , [arXiv:2402.13864](#).
- [22] H.-M. Chang, M. Procura, J. Thaler, and W. J. Waalewijn, *Calculating Track-Based Observables for the LHC*, *Phys. Rev. Lett.* **111** (2013) 102002, [[arXiv:1303.6637](#)].
- [23] H.-M. Chang, M. Procura, J. Thaler, and W. J. Waalewijn, *Calculating Track Thrust with Track Functions*, *Phys. Rev.* **D88** (2013) 034030, [[arXiv:1306.6630](#)].
- [24] J. C. Collins, D. E. Soper, and G. F. Sterman, *Factorization of Hard Processes in QCD*, *Adv. Ser. Direct. High Energy Phys.* **5** (1989) 1–91, [[hep-ph/0409313](#)].
- [25] Y. Li, I. Moutl, S. S. van Velzen, W. J. Waalewijn, and H. X. Zhu, *Extending Precision Perturbative QCD with Track Functions*, *Phys. Rev. Lett.* **128** (2022), no. 18 182001, [[arXiv:2108.01674](#)].
- [26] M. Jaarsma, Y. Li, I. Moutl, W. Waalewijn, and H. X. Zhu, *Renormalization group flows for track function moments*, *JHEP* **06** (2022) 139, [[arXiv:2201.05166](#)].
- [27] H. Chen, M. Jaarsma, Y. Li, I. Moutl, W. J. Waalewijn, and H. X. Zhu, *Collinear Parton Dynamics Beyond DGLAP*, [arXiv:2210.10061](#).
- [28] H. Chen, M. Jaarsma, Y. Li, I. Moutl, W. J. Waalewijn, and H. X. Zhu, *Multi-Collinear Splitting Kernels for Track Function Evolution*, [arXiv:2210.10058](#).
- [29] J. C. Collins and D. E. Soper, *Back-To-Back Jets in QCD*, *Nucl. Phys. B* **193** (1981) 381. [Erratum: *Nucl.Phys.B* 213, 545 (1983)].
- [30] M.-x. Luo, T.-Z. Yang, H. X. Zhu, and Y. J. Zhu, *Unpolarized quark and gluon TMD PDFs and FFs at N^3LO* , *JHEP* **06** (2021) 115, [[arXiv:2012.03256](#)].